Computational Insights on the Use of High Frequency Stimulation as a Nerve Conduction Block

Hunter J. Strathman, Michael D. Paskett, Alan D. Dorval

***Abstract*—Neuropathic pain can be a debilitating condition which negatively impacts an individual's quality of life. Reducing neuropathic pain through high-frequency, alternating-current (HFAC) stimulation has been explored as a method of blocking neuropathic pain without blocking other needed efferent and afferent communication with the central nervous system (e.g., motor control, proprioception) [1]–[3]. The exact mechanism of the conduction block is unknown; however, some argue that the source of the block is due to unintended direct current contamination through unbalanced sinusoidal waveform generation [4]. Direct current stimulation is undesirable as it may induce irreversible faradaic reactions at the interface between the electrode and tissue; these faradaic reactions can lead to electrode dissolution, free-radical generation, gas production, affect neural activity and cause nerve damage [5].**

In this work, we modeled myelinated and unmyelinated axons of various sizes (1 - 16 μm) and simulated several HFAC (2-16 kHz) and direct-current stimulation paradigms to investigate the efficacy of HFAC stimulation and the likelihood of direct-current contamination from a computational perspective. Our results suggest that HFAC stimulation is sufficient to induce conduction block with no DC offset at the electrode or stimulation source. Myelinated axons were found to require less current than unmyelinated to induce the block and displayed a non-linear relationship between frequency and stimulation current required to induce a block, specifically at lower frequencies.

I. Introduction

Neuropathic pain can be a debilitating condition which negatively impacts an individual's quality of life. Treatments for neuropathic pain range from pharmacologic to surgical intervention, and success outcomes are inconsistent. Thus, there exists a clinical need for a reliable method of treating neuropathic pain. Bioelectronic medicine may provide relief for debilitating neuropathic pain.

Neural signals can be blocked through applying electrical currents in the proximity of the nerve, preventing painful afferent signals from reaching the central nervous system and causing painful percepts. It has previously been demonstrated that applying direct current to nerve fibers is capable of producing a conduction block [1]. However, applying unbalanced currents to the nerve is undesirable as the accumulation of charge may cause irreversible faradaic reactions [2], [3], degrade the electrode, produce gas, or generate free radicals [4].

H.J. Strathman, M.D. Paskett and A.D. Dorval are with the Biomedical Engineering Department, University of Utah, Salt Lake City, UT 84112 USA. (e-mail: h.strathman@utah.edu; michael.paskett@utah.edu; chuck.dorval@utah.edu)

High-frequency, alternating current (HFAC) injection has been investigated as a charge-balanced method of blocking neuropathic pain without blocking other needed efferent and afferent communication between the central nervous system and the periphery (e.g., motor control, proprioception) [5]–[7]. The exact mechanism of the conduction block is unknown; however, some argue that the source of the block is due to unintended direct current contamination through unbalanced sinusoidal waveform generation [8], an undesirable mechanism.

In this work, we modeled myelinated and unmyelinated axons of various sizes (1 - 16 μm) and simulated several HFAC (2-16 kHz) and direct-current stimulation paradigms to investigate the efficacy of HFAC stimulation and the likelihood of direct-current contamination from a computational perspective.

II. Methods

A. Axon Models

All axons were modeled with a length of approximately 1 cm using the Hodgkin Huxley parameters shown in Table 1. Unmyelinated axons were modeled with 100 compartments using 1 and 2 μm diameters. Myelinated axons were modeled with 10 compartments using 2, 4, 8, and 16 μm diameters.

Action potentials were initiated at one end of the axon using the intracellular current necessary to produce repeated action potentials. Extracellular stimulation was simulated at the middle compartment using direct current and HFAC (2, 4, 8, and 16 kHz) stimulation. Stimulation amplitudes were increased until an effective conduction block was established, or the stimulation artifact in the middle compartment exceeded the amplitude of the action potential.

TABLE I. Model Parameters

Parameter	Value
Length	1 cm
Membrane Capacitance	10 fF/μm^2
Internal Resistance	1x10^{-6} TΩ μm
Potassium Conductance	360 pS/μm^2
Sodium Conductance	1900 pS/μm^2
Leaky Conductance	3 pS/μm^2
Potassium Reversal Potential	-77 mV
Sodium Reversal Potential	50 mV
Leaky Reversal Potential	-54.4 mV

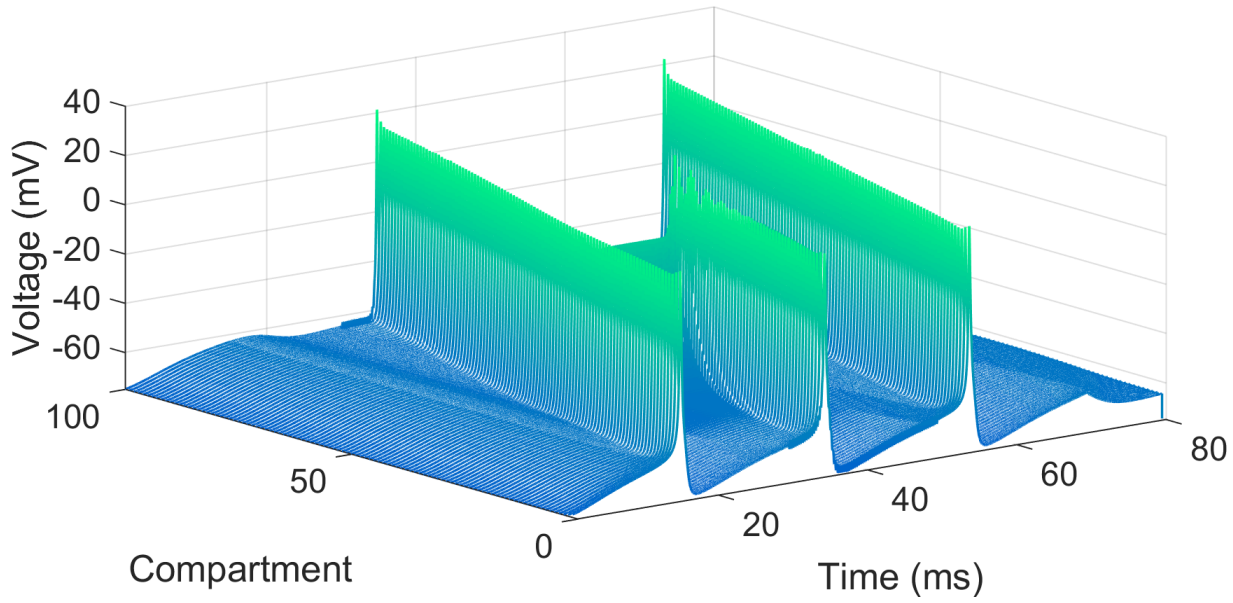

Figure 1. Exemplary conduction block of simulated 2 µm diameter unmyelinated axon. Axon consisted of 100 compartments. Excitatory stimulation was delivered from 0 – 70 ms, and a 4 kHz, 8.2 mA blocking stimulation applied 400 µm from compartment 50 from 20 – 50 ms. Action potential is initiated in compartment 0 and travels to compartment 100. Conduction block is clearly visible from compartment 50 – 100 above, while remaining intact in compartments 0 – 49. A third action potential can be seen near 55 ms after the block is removed.

B. Extracellular Field Potential Calculation

Extracellular field potentials were calculated based on the distance of the electrode (point source) to the center of the compartment based on the following equation:

$$V(r) = \frac{I}{4\pi\sigma r} \quad (1)$$

where V is the extracellular voltage, r is the distance from the electrode to the center of the compartment, I is the injected current, and σ is the is the conductivity of the medium (3.33×10^{-3} S/cm).

For unmyelinated axon models, the extracellular potential was calculated for each of the 100 µm compartments. For myelinated axons, the axon was broken down into 1 µm compartments, and down-sampled for every 1000th compartment, to represent ~ 1 mm myelin sheaths and 1 µm nodes of Ranvier.

C. ODE Simulations

All models were solved using MATLAB R2018a. The ODE15s ODE solver was used for calculating the changes in membrane potential, and the m, h, and n gates. Specifically, the ODE solver used Eqn. 2 below:

$$\frac{dV}{dt} = \left(\begin{array}{c} (G_{Na}(V_{Na} - V_{IN}) + G_K(V_K - V_{IN}) + \\ G_L(V_L - V_{IN}) + \frac{(V_{IN-1} - V_{IN})}{R_i} + \\ \frac{(V_{IN+1} - V_{IN})}{R_i} \end{array} \right) \Big/ Cm \quad (2)$$

where G_{Na}, G_K and G_L are the conductance for sodium, potassium and leak channels respectively, calculated from the following equations:

$$G_{Na} = g_{Na} A m^3 h$$
$$G_K = g_K A n^4$$
$$G_L = g_L A$$

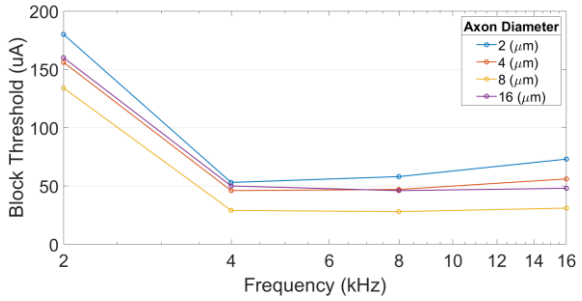

Figure 2. Conduction block thresholds for HFAC stimulation applied to myelinated axons. Stimulation thresholds calculated at 2, 4, 8 and 16 kHz for each axon diameter.

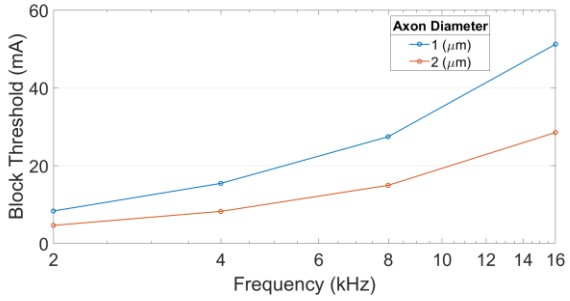

Figure 3. Conduction block thresholds for HFAC stimulation applied to unmyelinated axons. Stimulation thresholds calculated at 2, 4, 8 and 16 kHz for each axon diameter.

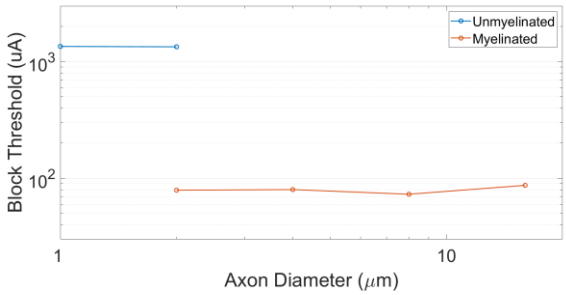

Figure 4. Conduction block thresholds for DC stimulation applied to myelinated and unmyelinated axons. 1 and 2 µm axon diameters tested for unmyelinated; 2, 4, 8 and 16 µm tested for myelinated.

The maximum step size of the ODE solver was set to 0.01 ms or 1/10th of the period of the HFAC stimulation, whichever was smaller. The absolute tolerance was set to 1x10^{-6}, and the relative tolerance was set to 1x10^{-6}.

III. Results

To determine the clinical utility of HFAC stimulation as a nerve conduction block, we tested the ability of pure AC stimulation to initiate a conduction block in simulated myelinated and unmyelinated axons. We also wanted to explore possible mechanisms for the selective conduction blocks seen in Duncan et al. [5], so we simulated axons at multiple physiological diameters.

Axon conduction block was successful at all tested frequencies, including DC, for both unmyelinated and myelinated axons. Fig. 1 shows an exemplary result for 4 kHz stimulation of an unmyelinated axon. It is clear from the figure that action potential propagation was blocked for all compartments distal to the stimulated region (compartment 50). Then, once the block was removed, a new action potential initiated post-block was able to pass unobstructed.

A. HFAC Stimulation of Myelinated Axons

Fig. 2 shows the relationship between axon diameter, AC stimulation frequency and block threshold. We were able to successfully initiate a conduction block for all simulated frequencies between 2 and 16 kHz. From 4 to 16 kHz, there was a slight increase in the amount of current required to initiate the conduction block with increasing frequency for all axon diameters except at 16 µm which did not show a clear trend.

There does not appear to be any clear relationship between stimulation threshold and axon diameter. Fig. 2 shows a general decrease in stimulation threshold across all frequencies for the increase in diameter from 2 to 4 µm, however, the 16 µm axon was found to have a block threshold somewhere between these two for all frequencies below 16 kHz. Interestingly, the 8 µm axon had the lowest stimulation threshold for all measured frequencies.

As seen in Fig. 2, all axon diameters showed an approximate 3-fold increase in stimulation threshold from 4 to 2 kHz. This is an interesting result that appears to be unique to the myelinated model.

B. HFAC Stimulation of Unmyelinated Axons

We successfully blocked action potential propagation for 1 and 2 µm unmyelinated axons. As seen in Fig. 3, we found the stimulation required to produce a conduction block increased proportional to the stimulating frequency. 2 µm axon models required approximately one half of the current of a 1 µm model to block action potential propagation indicating an inverse relationship between axon size and stimulation required for conduction block.

C. DC Conduction Block

We found, contrary to our previous simulations using HFAC stimulation, that there was little difference in the current required to induce a DC conduction block in unmyelinated axons of both sizes (1 and 2 µm; Figure 4). We had a similar result for myelinated axons of different sizes (2, 4, 8, and 16 µm). Unmyelinated axon conduction block thresholds were about an order of magnitude greater than myelinated axons.

IV. Discussion

We were able to successfully simulate conduction blocks in myelinated and unmyelinated axons from both DC and AC stimulation paradigms. In general, myelinated models required much less current to produce a conduction block. Interestingly, we found the relationship between stimulation frequency and block threshold to be highly nonlinear in myelinated axons. Our simulations show that larger axons are activated at lower thresholds of stimulation.

From our modeling, we were unable to find support for the conduction block selective to nociceptive fibers (unmyelinated fibers, roughly 1 µm) from Duncan et. al [5]. Based on our results, enough current was injected to produce an intrafascicular conduction block; however, as the Duncan et. al study stimulated 12-17 electrodes, the resultant potential fields are difficult to interpret. We hypothesize that the dramatic increase in stimulation threshold seen at 2 kHz for all tested diameters of myelinated axons could be related to the results seen in vivo. While the amplitudes, even at 2 kHz, are approximately 20x lower than the threshold seen for the same diameter (see 2 µm) unmyelinated axon, this presents a possible trend that may be more (or less) significant in a physiological environment.

Based on our simulations, it seems plausible that DC artifact could be part of the block phenomenon seen with HFAC stimulation. Our models indicate that the threshold for conduction block of unmyelinated axons are much lower for DC than HFAC stimulation, thus making any DC contamination of a HFAC more likely to be the source of the conduction block. We urge further studies using HFAC stimulation to ensure the output simulations are properly charge-balanced.

References

[1] N. Bhadra and K. L. Kilgore, "Direct current electrical conduction block of peripheral nerve," *IEEE Trans. Neural Syst. Rehabil. Eng.*, vol. 12, no. 3, pp. 313–324, 2004.

[2] D. B. McCreery, W. F. Agnew, T. G. H. Yuen, and L. A. Bullara,

"Comparison of neural damage induced by electrical stimulation with faradaic and capacitor electrodes," *Ann. Biomed. Eng.*, vol. 16, no. 5, pp. 463–481, Sep. 1988.

[3] W. F. Agnew and D. B. McCreery, "Considerations for safety with chronically implanted nerve electrodes.," *Epilepsia*, vol. 31 Suppl 2, pp. S27-32, 1990.

[4] S. F. Cogan, "Neural Stimulation and Recording Electrodes," *Annu. Rev. Biomed. Eng.*, vol. 10, no. 1, pp. 275–309, Aug. 2008.

[5] C. C. Duncan *et al.*, "Selective Decrease in Allodynia With High-Frequency Neuromodulation via High-Electrode-Count Intrafascicular Peripheral Nerve Interface After Brachial Plexus Injury," *Neuromodulation*, vol. 2018, 2018.

[6] K. L. Kilgore and N. Bhadra, "Reversible nerve conduction block using kilohertz frequency alternating current," *Neuromodulation*, vol. 17, no. 3, pp. 242–254, 2014.

[7] A. Soin, N. Syed Shah, and Z.-P. Fang, "High-Frequency Electrical Nerve Block for Postamputation Pain: A Pilot Study," *Neuromodulation Technol. Neural Interface*, vol. 18, no. 3, pp. 197–206, 2015.

[8] M. Franke, N. Bhadra, N. Bhadra, and K. Kilgore, "Direct current contamination of kilohertz frequency alternating current waveforms," *J. Neurosci. Methods*, vol. 232, pp. 74–83, 2014.